Rutgers Astrophysics Preprint #488, Submitted to ApJ
Preprint typeset using LaTeX style emulateapj

HALO DENSITY REDUCTION BY BARYONIC SETTLING?

J. R. Jardel

and

J. A. Sellwood
Rutgers University, Department of Physics & Astronomy,
136 Frelinghuysen Road, Piscataway, NJ 08854-8019
jjardel:sellwood@physics.rutgers.edu

Rutgers Astrophysics Preprint #488, Submitted to ApJ

ABSTRACT

We test the proposal by El-Zant *et al.* that the dark matter density of halos could be reduced through dynamical friction acting on heavy baryonic clumps in the early stages of galaxy formation. Using N-body simulations, we confirm that the inner halo density cusp is flattened to 0.2 of the halo break radius by the settling of a single clump of mass $\gtrsim 0.5\%$ of the halo mass. We also find that an ensemble of 50 clumps each having masses $\gtrsim 0.2\%$ can flatten the cusp to almost the halo break radius on a time scale of ~ 9 Gyr, for an NFW halo of concentration 15. We summarize some of the difficulties that need to be overcome if this mechanism is to resolve the apparent conflict between the observed inner densities of galaxy halos and the predictions of LCDM.

Subject headings: galaxies: evolution — galaxies: halos — galaxies: formation — galaxies: kinematics and dynamics

1. INTRODUCTION

The LCDM model for structure formation in the universe has been very successful on large scales (*e.g.* Springel, Frenk & White 2006), but has run into a number of difficulties on galaxy scales. One difficulty is that the predicted dark matter density in the halos of bright galaxies appears to be greater than that inferred from the best observational data (*e.g.* Weiner *et al.* 2001; Dutton *et al.* 2007) or from dynamical friction constraints (Debattista & Sellwood 2000); see Sellwood (2008b) for a review.

A number of possible solutions have been suggested. Binney, Gerhard & Silk (2001) and others suggest that the halo density can be reduced by feed-back from star formation, but Gnedin & Zhao (2002) show that the density cannot be reduced by more than a factor two, even for the most extreme feedback, unless the baryons are unreasonably concentrated. Weinberg & Katz (2002) propose that dynamical friction between a bar and the halo can reduce the central density, but Sellwood (2008a) shows that significant reductions require extreme bars and remove a large fraction of the angular momentum from the baryons.

A third possible solution was proposed by El-Zant, Shlosman & Hoffman (2001, hereafter EZ01), who suggested that dynamical friction between heavy gas clumps and dark matter would transfer energy to the dark matter, thereby reducing its inner density.

Essentially EZ01 propose a process of mass segregation that allows the baryonic matter to displace the dark matter. If it works, it would amount to baryon settling with halo *de*-compression, as Dutton *et al.* (2007) argued would be required to improve agreement of LCDM predictions with scaling relations of $\sim L_*$ galaxies. Kassin, de Jong & Weiner (2006) also remark that rotation curves could be more easily reconciled with LCDM predictions if halo compression could somehow be avoided. Tonini, Lapi & Salucci (2006) use the idea to predict rotation curves for galaxies. Mo & Mao (2004) apply the mechanism to preprocess small halos in the very early stages of structure formation.

A similar, but significantly distinct, idea was tested by Gao *et al.* (2004), who argue that some unspecified attractor mechanism causes violent relaxation processes to reset the collisionless mass profile of the combined dark and baryonic matter. Since violent mergers disrupt disks, Gao *et al.* clearly invoke a different process from the slow frictional in-spiral of baryonic clumps proposed by EZ01.

EZ01 suppose that the baryons collect into dense mass clumps which then sink to the center by dynamical friction. They assume: (1) the clumps are small enough they do not collide and (2) are sufficiently tightly bound that they are not tidally disrupted. They also implicitly assume that the dense clumps (3) maintain their coherence independent of any internal physical processes (such as possible star formation) and (4) they require the mass clumps to contain little dark matter.

The in-spiral of massive clumps has been studied extensively and we do not attempt a complete list of references. Van den Bosch *et al.* (1999) estimate the infall rate of dark matter sub-clumps through dynamical friction. Ma & Boylan-Kolchin (2004) simulate a mass spectrum of satellites each composed of particles moving within a main halo; they find that the combined density profile of the inner halo and disrupted satellites can either steepen or flatten, depending on the properties of the clumps. Arena & Bertin (2007) study both the strength of the friction force and the effect on the density profile for both cuspy and cored initial galaxy profiles.

Here we undertake a direct test of the proposal by EZ01, using self-consistent N-body simulations, in order to determine the clump mass required to effect a significant density reduction. We first derive the settling time-scale for single massive clumps in cuspy halos, and then present simulations containing an ensemble of heavy clumps in a background of light halo particles. We discuss the physical plausibility of their assumptions in the concluding section.

El-Zant *et al.* (2004, hereafter EZ04) apply the same idea to account for the flattened density profile reported by Sand *et al.* (2002) in the galaxy cluster MS 2137-23. In this context, they identify the galaxies themselves as the heavy baryonic clumps that settle to the cluster center. Both they, and Nipoti *et al.* (2004), present simulations to show that the in-spiral of galaxies can cause the background dark matter density profile to flatten, although both studies neglect the DM halos attached to the infalling galaxies. In an appendix, we show that our simulations are in good agreement with those of EZ04 for the same problem.

2. MODEL AND METHOD

In this work we adopt the NFW halo density profile (Navarro, Frenk & White 1997):

$$\rho(r) = \frac{\rho_s r_s^3}{r(r+r_s)^2}, \tag{1}$$

where r_s and ρ_s respectively set the radius and density scales. Since the mass is logarithmically divergent at large radii, we adopt $M_* = 4\pi\rho_s r_s^3$ as a convenient mass scale; for reference, M_* is the mass enclosed within $r \simeq 5.305 r_s$ and the mass enclosed within a sphere of $15r_s$ is $\simeq 1.835 M_*$. An isotropic distribution function (DF) for the NFW halo can be obtained by Eddington inversion (Binney & Tremaine 2008, eq. 4-46). We limit the radial extent of the halo by eliminating all particles with energy $E > \Phi(r_{\rm max})$, where Φ is the gravitational potential of the untruncated halo and $r_{\rm max} = 15 r_s$.

In most of our work, we calculate the self-forces between the halo particles using a surface harmonic expansion on a spherical grid (Sellwood 2003). We employ a radial grid with 300 zones, and typically expand up to $l_{\rm max} = 4$ for the field of the halo particles. We recenter the spherical grid on the densest point in the halo at frequent intervals using the method described by McGlynn (1984). As Zaritsky & White (1988) find that results with this type of code can depend upon the recentering mechanism, we show in the appendix that results from our preferred method agree well with those using a Cartesian grid where recentering is not needed.

We augment the grid-determined acceleration of a light (halo) particle at position $\boldsymbol{r}$ by the attraction of N_h heavy, softened point masses at positions $\boldsymbol{r'}$:

$$\ddot{\boldsymbol{r}} = -G \sum_{N_h} M_h \frac{\boldsymbol{r} - \boldsymbol{r'}}{|\boldsymbol{r} - \boldsymbol{r'}|^3} g\left(\frac{|\boldsymbol{r} - \boldsymbol{r'}|}{\epsilon}\right), \tag{2}$$

where M_h is the mass of each heavy particle and ϵ the softening length. The acceleration of each heavy particle is

$$\ddot{\boldsymbol{r}}' = -G \sum_{N_l} M_l \frac{\boldsymbol{r}' - \boldsymbol{r}}{|\boldsymbol{r} - \boldsymbol{r'}|^3} g\left(\frac{|\boldsymbol{r} - \boldsymbol{r'}|}{\epsilon}\right), \tag{3}$$

where the summation is over all N_l light particles whose masses are M_l, plus the forces from all other heavy particles as given by eq. (2). This strategy is practicable as long as N_h is not too large.

In this work, we generally adopt a finite softening kernel, such that

$$g(x) = \begin{cases} x^3(5x^3 - 9x^2 + 5) & x < 1 \\ 1 & \text{otherwise,} \end{cases} \tag{4}$$

which is the attraction of a spherical cloud of mass m having the density profile $\rho(x) = 15m(2x^3 - 3x^2 + 1)/(4\pi\epsilon^3)$, that declines as a cubic function from a maximum at the center to zero at $x = 1$. For this kernel the attractive force peaks at $x \simeq 0.564$ and joins smoothly to the inverse square law at $x = 1$. For comparison with older work only, we have also used traditional Plummer softening of the form $g'(x) = x^3/(1 + x^2)^{3/2}$, which weakens forces at all separations. Values of ϵ for the cubic kernel should be larger than for the Plummer kernel, since attractive forces from equation (4) are substantially sharper.

Consistent with previous work, we use the term satellite to describe a single heavy particle orbiting within the halo. In this case, we set the satellite in a circular orbit at some initial radius, and share a net momentum in the opposite direction among the halo particles, such that the combined linear momentum of the system is zero.

We have verified that our results are insensitive to the time step, grid size, and halo particle number. The code conserves total energy and angular momentum to better than 0.2% and 0.05% respectively, while linear momentum variations never exceed $0.001(GM^3/r_s)^{1/2}$. As an additional check of our calculations, we reproduced the result for a "halo" represented by an $n = 3$ polytrope from Bontekoe & van Albada (1987). The settling time, using 200 times as many particles, agreed with their value to within their estimated error.

Henceforth, we adopt units such that $G = M_* = r_s = 1$. A numerically convenient scaling to physical units is to choose $M_* = 7.6 \times 10^{11}$ M$_\odot$ and $r_s = 15$ kpc, which sets the unit of time $(r_s^3/GM_*)^{1/2} = 30$ Myr. An NFW halo with these parameters has concentration $c \simeq 15$ and $V_{200} \simeq 134$ kms^{-1}; the time unit would be longer in lower concentration halos.

3. A SINGLE SATELLITE

We begin by revisiting the orbital decay of a single massive satellite. The problem of dynamical friction on a heavy particle orbiting in a spherical system of light particles has been worked on extensively. Our purpose here is simply to determine the settling time of a softened heavy particle in a cuspy halo, before going on to study the behavior of a collection of such particles in §4.

Our fiducial run uses a satellite of mass $M_h = 0.01 M_*$ with $\epsilon = 0.15 r_s$ in an NFW halo, with an initially circular orbit started at $r = 4r_s$. We represent the halo with 10^6 particles, use a grid with 300 radial shells, expand up to $l_{\rm max} = 4$ and employ a basic time step of $0.005(r_s^3/GM)^{1/2}$. While the decay rate of the satellite orbit is independent of most numerical parameters, it is marginally increased, by $\sim 1\%$, when we increase $l_{\rm max}$ to 10, and it also depends weakly on the softening length adopted for the satellite, as discussed below.

3.1. *Settling time*

Figure 1 (upper) shows the time evolution of the angular momentum of the satellite. The rate of loss due to dynamical friction accelerates as the satellite settles to the center at which point further change abruptly ceases. Thus it takes ~ 260 dynamical times, or 7.8 Gyr, for the satellite to settle to the center of the NFW halo from its initial radius. The settling time will be longer in lower density

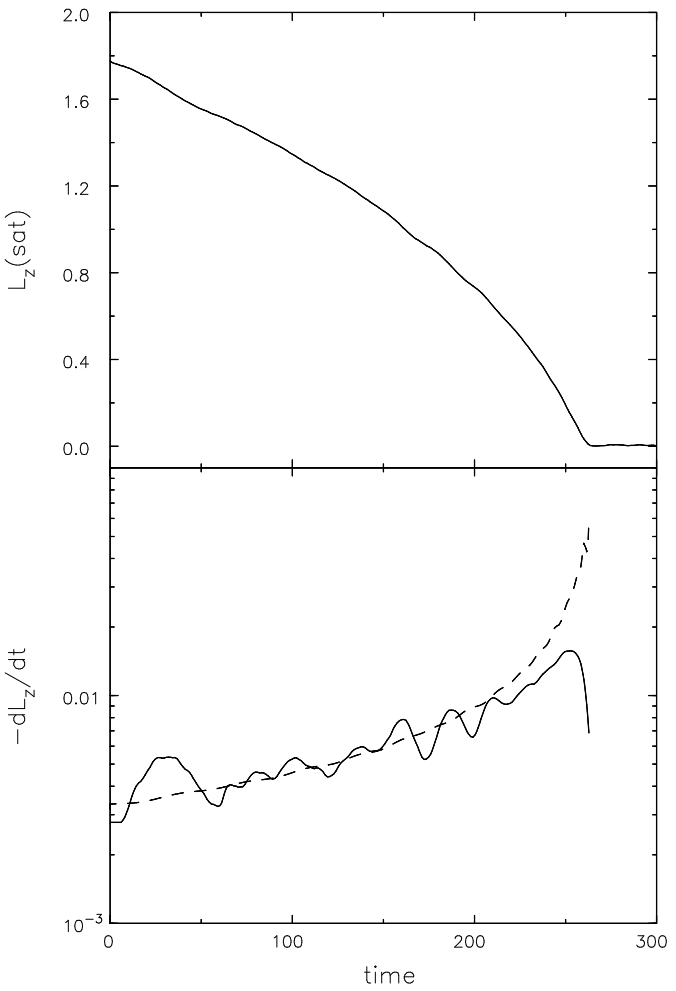

FIG. 1.— Above, the time evolution of the satellite's orbital angular momentum in the fiducial run. Below, the frictional torque measured from the simulation (solid) and predicted by eq. 5 (dashed) for $\ln\Lambda = 2.5$.

halos, or if the satellite starts farther out.

The well-known formula (Chandrasekhar 1943; Binney & Tremaine 2008) for the acceleration $\boldsymbol{a}_f$ of a heavy particle moving at velocity $\boldsymbol{v}$ through a sea of light particles of constant density ρ is

$$\boldsymbol{a}_f(v) = -\frac{\boldsymbol{v}}{v} 4\pi \ln\Lambda G^2 \frac{M_h \rho}{\sigma^2} V\left(\frac{v}{\sigma}\right). \qquad (5)$$

Here $v = |\boldsymbol{v}|$, $\ln\Lambda$ is the usual Coulomb logarithm and

$$V(x) = x^{-2}\left[\mathrm{erf}\left(\frac{x}{\sqrt{2}}\right) - \left(\frac{2}{\pi}\right)^{1/2} x e^{-x^2/2}\right]; \qquad (6)$$

the quantity in the square brackets is the fraction of light particles having speed $< v$, assuming the particles to have a Maxwellian velocity distribution with dispersion σ. While the assumptions made in the derivation of this formula do not strictly permit it to be applied to the present problem (*e.g.* Tremaine & Weinberg 1984), it correctly predicts the scaling with parameters (*e.g.* Lin & Tremaine 1983; Sellwood 2006; Arena & Bertin 2007).

The lower panel of Fig. 1 compares the prediction of formula (5) with our numerical results. The solid curve shows the rate of loss of angular momentum by the satellite, while the dashed curve shows the expected torque, $\boldsymbol{r}' \times \boldsymbol{a}_f$, using local values for the density and velocity dispersion of the halo particles.[1] We treat the Coulomb logarithm, which is not predicted with any certainty, as a free scaling parameter; the curve shown is for $\ln\Lambda = 2.5$. The agreement is satisfactory until the final plunge of the satellite, where the empirical torque drops below that predicted. We have verified that the frictional torque scales appropriately with the local density and velocity dispersion, and linearly with the mass of the heavy particle for $M_h \lesssim 0.05 M_*$.

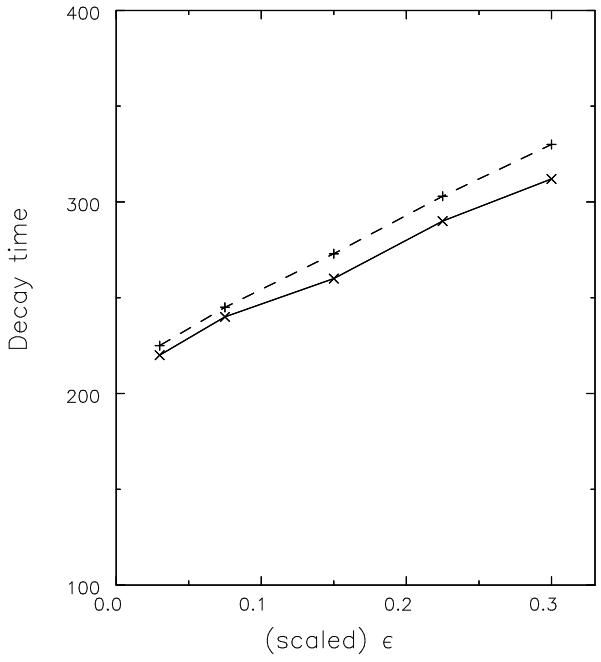

FIG. 2.— The variation of settling time with satellite softening length. Results using the cubic softening rule, eq. (4) (points joined by the solid line) are quite similar to those using a Plummer kernel with $\epsilon/3$ (dashed line).

The low value of $\ln\Lambda$ required to match our data is not purely a consequence of satellite softening. The solid line in Figure 2 shows that the time taken for a satellite of mass $M_h = 0.01$ to settle to the center from a circular orbit at $r = 4$ varies approximately linearly with softening length. As is reasonable, more concentrated satellites settle more rapidly, but the variation is by a factor ~ 1.5 for a factor ten change in the softening length, which is a somewhat slower dependence than $\ln\epsilon$. Low values of $\ln\Lambda$ are widely reported in other work (*e.g.* Boylan-Kolchin, Ma & Quataert 2007 and references therein), and are discussed in the appendix of Milosavljević & Merritt (2001).

Fig. 2 also compares the results using the cubic softening kernel (solid line) with those from the more traditional Plummer rule (dashed line). The results compare well when the Plummer softening length is about 1/3 that for the sharper cubic kernel. For both softening rules, we find the torque is reasonably well predicted by eq. (5) for the same $\ln\Lambda$ when ϵ is scaled by this factor.

[1] Measurement of the frictional torque offers a simpler and more direct comparison with eq. (5) than through the rate of energy loss used elsewhere (*e.g.* Bontekoe & van Albada 1987; Arena & Bertin 2007).

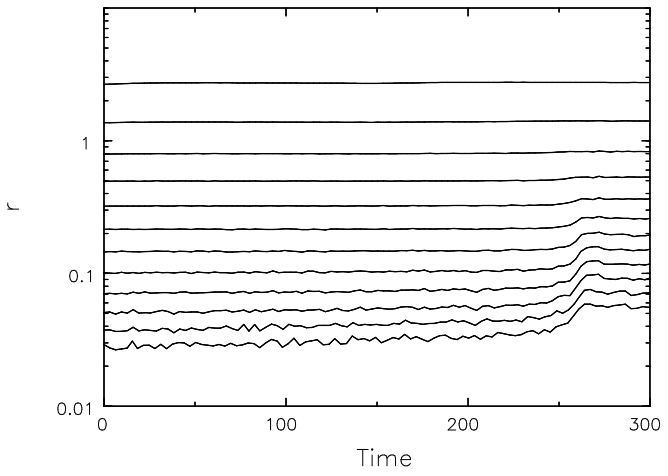

FIG. 3.— The time evolution of the Lagrangian radii in the fiducial run. Each curve shows the radius enclosing a fixed fraction of the halo mass, with the lowest curve corresponding to 2×10^{-4}, rising by a factor 2 at each subsequent trace. The changes are minor until the satellite enters the cusp.

We have run a small number of additional experiments with satellites on initially non-circular orbits. The Chandrasekhar friction formula (eq. 5) continues to predict the rate of angular momentum loss, with the same $\ln\Lambda$. Generally, the settling time when the orbit is not strongly eccentric is only slightly longer than that from a circular orbit with the same initial angular momentum. More eccentric orbits take longer to settle, because the satellite spends more time at radii well beyond its guiding center radius where the background density is lower. It should be noted that adding radial motion at fixed angular momentum, as we discuss here, increases the satellite's energy, so our conclusion remains consistent with other work (*e.g.* van den Bosch *et al.* 1999).

Our experiments have been confined to spherical dark matter halos, whereas halos are expected to be mildly triaxial (*e.g.* Jing & Suto 2002). A mass clump in a triaxial halo may pursue a box orbit (Binney & Tremaine 2008, ch. 3), causing it to pass through the dense center from time to time and possibly reducing the settling time (*e.g.* Pesce, Capuzzo-Dolcetta & Vietri 1992). However, such orbits are already eccentric and settle more slowly than quasi-circular orbits.

3.2. *Halo density changes*

As the satellite settles to the center, the halo particles are heated and the density of the inner halo decreases. Figure 3, from our fiducial run, shows the time evolution of the radii containing many different mass fractions, indicating that the mass profile undergoes little change until after time 250. These Lagrangian radii are always computed from a center at the densest point. Since the distance of the satellite from the center falls below r_s only after $t \sim 250$, most of the change to the mass profile of the halo occurs during the final plunge of the satellite through the cusp, in agreement with the conclusions of EZ01.

Figure 4 shows the density and mass profiles after the satellite has settled from the same initial orbit in each case. The changes are not large; the cusp is flattened inside

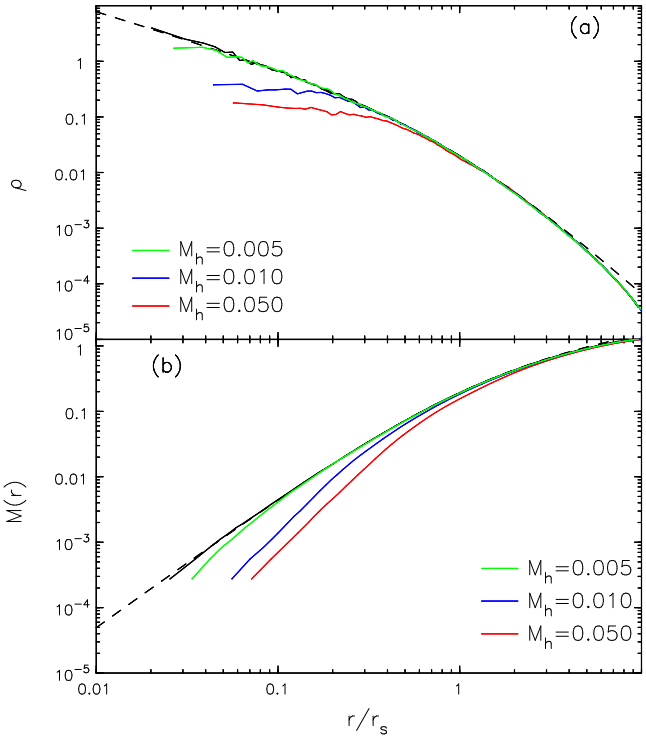

FIG. 4.— The changes in (a) density and (b) mass profile caused by the settling of a single satellite of 0.5%, 1% and 5% of the halo mass from an initially circular orbit at $r = 4rs$ in an NFW halo. The solid lines show the density or mass profiles measured from the particles at the start (black) and when the satellite has settled (color). The dashed lines show the corresponding theoretical NFW curves.

$r \lesssim 0.2r_s$ in our fiducial run (upper panel), where the satellite mass is $0.01M_*$ or $\gtrsim 0.5\%$ of the *halo* mass. The changes produced by heavier and lighter infalling masses differ in the expected sense. These measurements of the density and mass profiles are, at all times, from a center located at the densest point.

4. COLLECTION OF HEAVIES

Dark matter and baryons are well mixed in the early universe. As halos form, the relative distributions of the collisionless dark matter and the collisional baryonic component become more difficult to predict as shock heating, feedback from star formation, and cold inflows may all occur (*e.g.* Cattaneo *et al.* 2007). The typical expectation is that some 5%–15% of a total galaxy's mass is baryonic.

In their models, EZ01 parameterize the clump mass as M_{200}/η, where M_{200} is the total (baryonic plus dark) mass of the galaxy. If the baryon fraction is f and all the baryons are in equal mass clumps, the number of clumps is therefore $f\eta$. These authors use the Chandrasekhar dynamical friction formula to predict the rate at which energy is removed from the heavy clumps, which they add locally to the dark matter and adjust its mass profile in response to the energy added at each radius.

Here instead, we use N-body simulations with both heavy and light particles. Consistent with their assumptions, we treat the baryonic mass clumps as heavy softened particles and integrate their motion through the smooth background halo composed of light, collisionless particles.

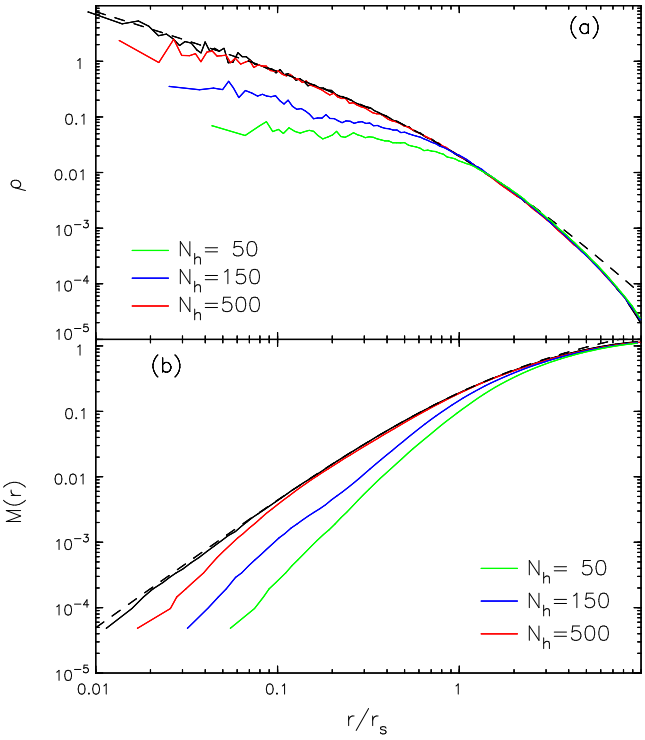

FIG. 5.— The changes in (a) density and (b) mass profile caused by the settling of N_h heavy particles with total mass of $0.1M_{200}$, initially distributed at uniform density within a sphere of radius $4rs$ in an NFW halo. The solid lines show the density or mass profiles measured from the particles at the start (black) and after 9 Gyr (color). The dashed lines show the corresponding theoretical NFW curves.

We first simulate their Model 1, which has a baryonic mass of 10% of the total enclosed within $15r_s$. In this model, the baryons are distributed uniformly inside a sphere of radius $r = 4r_s$, while the dark matter has an NFW distribution. We therefore redetermine the initial equilibrium DF for the halo, to take account of the additional central attraction caused by the baryonic matter. In our simulation, the dark matter is represented by 500 000 particles drawn from the new DF, while we set the isotropic initial velocities of the 500 equal-mass heavy particles using the procedure described by Hernquist (1993).

We find some density reduction of the inner NFW profile as the heavy particles settle. Figure 5 shows the density and mass profile of the light (dark matter) particles after 300 dynamical times, or ~ 9 Gyr. A small reduction of the dark matter density is achieved over this time when 500 heavy particles represent the entire baryonic mass ($f = 0.1$). Naturally, the effect is increased as the baryonic mass is concentrated into fewer, more massive particles, since each heavy particle experiences stronger friction and settles more quickly.

If the baryonic mass clumps are distributed as the dark matter, mass segregation is even slower. EZ01 find little evolution with $N_h = 500$ in an NFW halo with the heavies distributed as the NFW density profile, which we confirm in a simulation with this set-up. Again we observe more significant changes when we employ fewer, more massive heavy particles.

Ma & Boylan Kolchin (2004) also followed the evolution of a main NFW halo having a smooth mass distribution, together with ~ 1000 mass clumps having a spectrum of masses. The total mass of the clumps was 7.02%, with the most massive being 1.51%, of the main halo. They report that the density of the main halo was substantially reduced when all the mass clumps were included, but was much less affected in a separate calculation when the three most massive clumps, which each had masses $\gtrsim 1\%$ of the main halo, were excluded. This is in agreement with our finding (Fig. 5) that the halo density is reduced more as the masses of the individual heavy particles rise from 0.02% to 0.2% of the main halo.

5. DISCUSSION AND CONCLUSIONS

El-Zant *et al.* (2001) proposed that dynamicl friction on massive gas clumps could lead to the outward displacement of dark matter. They estimated the magnitude of the effect on a galaxy halo using the Chandrasekhar dynamical friction formula. They followed up (El-Zant *et al.* 2004) with simulations of a galaxy cluster, in which the heavy particles were the individual galaxies, finding some density decrease.

We present simulations of softened heavy particles moving under the influence of gravitational forces within a background NFW halo composed of a large number of light particles. We confirm that the inner halo density is lowered by dynamical friction on heavy particles, as has been found previously (*e.g.* Ma & Boylan-Kolchin 2004; Arena & Bertin 2007), and show that larger reductions result from more massive particles that also settle more rapidly.

We specifically test the model proposed by EZ01, who divided all the baryons into a number of equal mass clumps that were already somewhat concentrated towards the halo center. We find (Fig. 5) that the $\sim 10\%$ baryonic mass fraction must be entirely made up of $\lesssim 150$ equal clumps if the cusp in the dark matter is to be flattened to $r \lesssim r_s$ within 300 dynamical times, which scales to ~ 9 Gyr for a $c = 15$ halo.

The principal reason that we observe a more mild density reduction than predicted by EZ01 is that friction is significantly weaker than they assumed. They, and Tonini *et al.* (2006), adopted $\ln\Lambda \simeq \ln\eta \simeq 8.5$ whereas we find $\ln\Lambda \simeq 2.5$ (§3.1), which causes the mass clumps to settle 2-3 times more slowly than they assumed, with a corresponding reduction in the rate energy is given up to the halo.

More massive clumps both spiral in more rapidly and displace more dark matter (Fig. 4). Ma & Boylan-Kolchin (2004) presented a pair of simulations that revealed a much smaller density change when the three most massive clumps were eliminated compared with the result when they were retained. Thus substantial reductions of the inner halo density require just a few extremely massive clumps, assuming they are not disrupted as they settle.

The time scale, in years, varies as $\rho_s^{-1/2}$, and therefore would be longer in lower concentration halos. At higher redshifts, the orbital period is a fixed fraction of the age of the universe at a constant overdensity (since both scale as the square root of the density in an Einstein-de Sitter universe). While halo densities rise with redshift, their

relative over-densities are lower (*e.g.* Zhao *et al.* 2003), and therefore more massive clumps are required to have any effect in the time available; Mo & Mao (2004) invoke baryon clumps having 5% of the halo mass when $2 \lesssim z \lesssim 5$.

EZ04 argue that the same physical process applies to galaxies in clusters, and present supporting simulations. Again adopting their numerical model and assumptions, we confirm (Appendix) their result that the density cusp flattens for $r \lesssim 0.2 r_s$, where we also demonstrate that the result is independent of the numerical method.

The physical assumptions underlying these successes are more questionable, however. Purely baryonic gas clumps are indeed expected to form through the Jeans instability as gas cools and settles in the main halo (*e.g.* Maller & Bullock 2004), but the high-resolution experiments of Kaufmann *et al.* (2006) show that gas fragments formed in this way have masses ranging up to $\sim 10^6$ $M_\odot$ only, some two orders of magnitude smaller than required to have interestingly short settling times.

Dark matter sub-halos (*e.g.* Diemand, Kuhlen & Madau 2007) may contain gas and would spiral in more rapidly. However, settling of such sub-halos would bring both baryons and DM into the center, diluting the desired separation of baryons from dark matter. The resulting changes to the overall dark matter density profile will clearly be less substantial. When Ma & Boylan-Kolchin (2004) treat sub-clumps as collections of particles, they find that the stripped mass is added to the main DM halo in such a way as approximately to replace the mass scattered to larger radii by dynamical friction. (The net effect can be either a small increase or decrease in the inner dark matter density, depending on the clump mass spectrum.) If dynamical friction is to separate the baryons from dark matter with the desired efficiency, baryonic mass clumps in sub-halos must somehow be stripped of their dark matter with high efficiency, without dissolving the gas clumps themselves.

In the case of the cluster simulation, EZ04 describe the heavy particles as purely baryonic galaxies. Here again, the change in the central dark matter density will not be as substantial when the dark halos of the galaxies are taken into account, as also noted by Nipoti *et al.* (2004).

Additional density reduction would be possible if massive baryonic clumps in the center of the halo could be re-accelerated. Models of this kind have been proposed by Mashchenko, Couchman & Wadsley (2006, 2007), who invoke star formation activity, and by Peirani, Kay & Silk (2008), who use AGN jets. It should be noted, however, that massive clumps of dense gas are not easily accelerated by these astrophysical processes (*e.g.* MacLow & Ferrara 1999). The rapid density reduction reported by Mashchenko *et al.* (2006) occurs because they employed a gas clump of 10^8 $M_\odot$ within the cusp driven sinusoidally with a bulk speed that peaked at 18 km s^{-1}.

Most halo density reduction occurs as clumps plunge rapidly within the cusp (Fig. 3), as noted by EZ01. Therefore, clumps that start out in the cusp fall in more rapidly and are most efficient at displacing the dark matter. However, only a small fraction ($\lesssim 5\%$) of the baryons start out in the cusp, if they are distributed as the dark matter. The desired halo density reduction would be more rapid if the baryonic fraction in the cusp could be increased, but it is hard to see how such an initial mass segregation could have arisen without compressing the halo.

Thus the challenge, if the proposal by EZ01 is to help solve the central density problem of dark matter halos, is to find ways to collect gas into clumps exceeding $\sim 0.5\%$ of the halo mass that can settle as coherent entities into the center.

We thank Kristine Spekkens and Frank van den Bosch for helpful comments on a draft of this paper. An anonymous referee and the editor, Chung-Pei Ma, also made constructive suggestions for improvement. This work was supported by grants AST-0507323 from the NSF and NNG05GC29G from NASA.

REFERENCES

Arena, S. E. & Bertin, G. 2007, A&A, **463**, 921
Binney, J., Gerhard, O. & Silk, J. 2001, MNRAS, **321**, 471
Binney, J. & Tremaine, S. 2008, *Galactic Dynamics* 2nd edition (Princeton: Princeton University Press)
Bontekoe, Tj. R. & van Albada, T. S. 1987, MNRAS, **224**, 439
Boylan-Kolchin, M., Ma, C-P. & Quataert, E. 2007, astro-ph/0707.2960
Cattaneo, A., Blaizot, J., Weinberg, D. H., Kereš, D., Colombi, S., Davé, R., Devriendt, J., Guiderdoni, B. & Katz, N. 2007, MNRAS, **377**, 63
Chandrasekhar, S. 1943, ApJ, **97**, 255
Debattista, V. P. & Sellwood, J. A. 2000, ApJ, **543**, 704
Diemand, J., Kuhlen, M. & Madau, P. 2007, ApJ, in press (astro-ph/0703337)
Dutton, A. A., van den Bosch, F. C., Dekel, A. & Courteau, S. 2007, ApJ, **654**, 27
El-Zant, A., Shlosman, I. & Hoffman, Y. 2001, ApJ, **560**, 636 (EZ01)
El-Zant, A., Hoffman, Y., Primack, J., Combes, F. & Shlosman, I. 2004, ApJ, **607**, L75 (EZ04)
Gao, L., Loeb, A., Peebles, P. J. E., White, S. D. M. & Jenkins, A. 2004, ApJ, **614**, 17
Gnedin, O. Y. & Zhao, H.S., 2002, MNRAS, **333**, 299
Hernquist, L. 1993, ApJS, **86**, 389
Jing, Y. P. & Suto, Y. 2002, ApJ, **574**, 538
Kassin, S. A., de Jong, R. S. & Weiner, B. J. 2006, ApJ, **643**, 804
Kaufmann, T., Mayer, L., Wadsley, J., Stadel, J. & Moore, B. 2006, MNRAS, **370**, 1612
Lin, D. N. C. & Tremaine, S. 1983, ApJ, **264**, 364
Ma, C-P. & Boylan-Kolchin, M. 2004, Phys. Rev. Lett., **93**, 21301
MacLow, M-M. & Ferrara, A. 1999, ApJ, **513**, 142
Maller, A. H. & Bullock, J. S. 2004, MNRAS, **355**, 694
Mashchenko, S., Couchman, H. M. P. & Wadsley, J. 2006, Nature, **442**, 539
Mashchenko, S., Couchman, H. M. P. & Wadsley, J. 2007, Science, **319**, 174
McGlynn, T. A. 1984, ApJ, **281**, 13
Milosavljević, M. & Merritt, D. 2001, ApJ, **563**, 34
Mo, H.-J. & Mao, S. 2004, MNRAS, **353**, 829
Navarro, J. F., Frenk, C. S. & White, S. D. M. 1997, ApJ, **490**, 493
Nipoti, C., Treu, T., Ciotti, L. & Stiavelli, M. 2004, MNRAS, **355**, 1119
Peirani, S., Kay, S. & Silk, J. 2008, A&A, **479**, 123
Pesce, E., Capuzzo-Dolcetta, R. & Vietri, M. 1992, MNRAS, **254**, 466
Sand, D. J., Treu, T. & Ellis, R. S. 2002, ApJ, **574**, L129
Sellwood, J. A. 2003, ApJ, **587**, 638
Sellwood, J. A. 2006, ApJ, **637**, 567
Sellwood, J. A. 2008a, ApJ, **679**, 379
Sellwood, J. A. 2008b, in "The Galaxy Disk in Cosmological Context" IAU Symp. **254**, eds. J. Andersen, J. Bland-Hawthorn & B. Nordström, (to appear) (arXiv:0807.1973)
Sellwood, J. A. & Merritt, D. 1994, ApJ, **425**, 530
Springel, V., Frenk, C. S. & White, S. D. M 2006, Nature, **440**, 1137
Stanford, S. A., Eisenhardt, P. R., Dickinson, M., Holden, B. P. & De Propris, R. 2002, ApJS, **142**, 153
Tonini, C., Lapi, A. & Salucci, P. 2006, ApJ, **649**, 591
Tremaine, S. & Weinberg, M. D. 1984, MNRAS, **209**, 729
van den Bosch, F. C., Lewis, G. F., Lake, G. & Stadel, J. 1999, ApJ, **515**, 50
Weinberg, M. D. & Katz, N. 2002, ApJ, **580**, 627
Weiner, B. J., Sellwood, J. A. & Williams, T. B. 2001, ApJ, **546**, 931
Zaritsky, D. & White, S. D. M. 1988, MNRAS, **235**, 289
Zhao, D. H., Jing, Y. P., Mo, H. J. & Börner, G. 2003, ApJ, **597**, L9

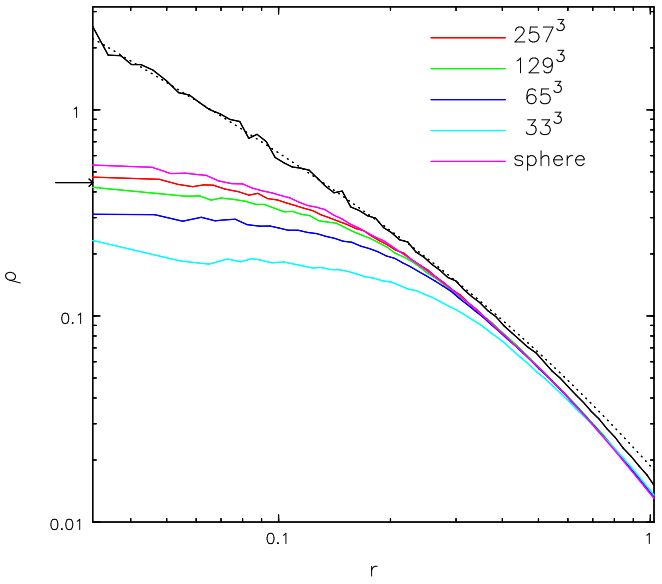

FIG. A6.— The initial (black) and final (color) density profiles of runs for comparison with EZ04, showing a converge test with four different Cartesian grids and our spherical grid (magenta). The core density obtained by EZ04 is marked by the arrow.

APPENDIX

GALAXY CLUSTER SIMULATIONS

El-Zant *et al.* (2004) present results from simulations using a non-adaptive Cartesian grid covering only the inner part of the dark matter halo of a cluster of galaxies. They report that the density of dark matter declined significantly at radii $< r_s/3$ of the NFW halo profile after ~ 10 Gyr. The numerical tests reported in this appendix reproduce their calculation.

Since EZ04 employed a 256^3 Cartesian grid, they restricted their calculation to the inner part of the NFW halo. They set the scale radius $r_s = 39$ mesh spaces, which implies that particles beyond a radius $r = 128r_s/39 \simeq 3.28r_s$ could lie outside the grid. They therefore truncate the NFW halo at $r = 3.33r_s$ and use a monopole approximation to integrate the motion of particles when they are off the grid. Their fiducial simulation uses 9×10^5 particles to represent the diffuse dark matter, and 90 heavy particles to represent galaxies, which collectively have a mass that is 6% of the total. Both the dark matter particles and the heavy particles have initially the same spatial extent and isotropic velocities.

In their calculation, all forces were computed using the grid. Forces from a point mass on a Cartesian grid (shown graphically in the appendix of Sellwood & Merritt 1994) resemble those from the cubic spline kernel (eq. 4) with a softening length of three grid spaces, or in their case $\epsilon \simeq 3r_s/39$.

Here we reproduce this calculation using our own 3-D Cartesian grid code (Sellwood & Merritt 1994), demonstrate numerical convergence, and compare results from this grid with those from our spherical grid. As EZ04, we place all particles, both heavy and light, on the 257^3 grid where we set $r_s = 40$ mesh spaces. When using other grids we compute interactions between the heavy particles (galaxies) and the light particles (dark matter) using the expressions (2) & (3), in order to preserve a constant softening length in physical units ($\epsilon = 0.075r_s$). We repeated the calculation with the same physical set-up using grids of size 33^3, 65^3, & 129^3 to compute the self-interactions of the light particles, with the physical length scale $r_s = 5$, 10, & 20 mesh spaces respectively.

The results are shown in Figure A6; the initial density profile is shown by the black line, the profiles after ~ 10 Gyr on the various grids are shown by the colored lines. (The colored lines show time averages over an interval of ±0.13 Gyr, in order to obtain smooth curves.) The magenta line in Fig. A6 also shows the result using the same physical model, but calculated using our high-resolution spherical grid. It is clear that the density reduction diminishes as the Cartesian mesh is refined, although the final density profile has almost converged at 257^3 and, reassuringly, this result agrees quite closely with that from our spherical grid. Furthermore, the final central density we obtain is very similar to that found by EZ04; the inner density in their model flattens to the value marked by the arrow.

We note that the results shown in Fig. A6 can be compared with $N_h = 150$ curve in Fig. 5. The masses of the individual heavy particles are 0.67×10^{-3} of the halo in both cases, but the halo concentrations differ, which affects the scaling with time. Since $c = 5.45$ for the cluster and $c = 15$ for the galaxies, the square root of the density ratios is ≈ 3.4. Therefore the cluster simulation is run for about one third the number of dynamical times of the galaxy, which also has more heavy particles. A comparison of the density profiles in the two simulations at equal numbers of dynamical times reveals very similar density changes, as it should.

Thus we confirm that a density reduction can indeed be obtained if the assumptions made by EZ04 hold. However, they invoke 90 massive galaxies in the inner part of the cluster, whereas the true number is probably less (Stanford *et al.* 2002). Furthermore they implausibly assume that the galaxies (heavy particles) have no dark halos, as acknowledged by Nipoti *et al.* (2004); more massive heavy particles will experience stronger friction, but as some dark matter is likely to be stripped from each galaxy's halo, the change to the overall dark matter profile needs to be computed from more realistic simulations (*e.g.* Ma & Boylan-Kolchin 2004).